

Supplementary Information for

Branching Crisscross Polymerization of Single-Stranded DNA Slats

Jie Deng^{a,b,c,d}, Dionis Minev^{a,b,c,e}, Anastasia Ershova^{a,b,c}, and William M. Shih^{*a,b,c}

a. Department of Cancer Biology, Dana-Farber Cancer Institute, Boston, MA, USA.

b. Wyss Institute for Biologically Inspired Engineering at Harvard University, Boston, MA, USA.

c. Department of Biological Chemistry and Molecular Pharmacology, Harvard Medical School, Boston, MA, USA.

d. Current address: School of Chemistry and Chemical Engineering, Huazhong University of Science and Technology, Wuhan, China.

e. Current address: CATALOG, Boston, MA, USA.

Email: William_Shih@dfci.harvard.edu

Materials

Instrumentation: Transmission electron microscopy (TEM) (JEOL JEM-1400Plus), thermal cycler (Bio-Rad), gel electrophoresis power supplies (Bio-Rad), vertical gel electrophoresis system (XCell Surelock minicell, Thermo Fisher Scientific), mini gel horizontal electrophoresis system (Thermo Fisher Scientific), Typhoon FLA 9500 gel scanner (GE Healthcare), Refrigerated Centrifuge (Eppendorf 5417R), and Nanodrop 2000c UV–Vis spectrophotometer (Thermo Fisher Scientific).

Reagents: All oligonucleotides with standard desalting were supplied by Integrated DNA Technologies Inc. (IDT), and the sequences are shown in the Supplementary Table. Unless otherwise mentioned, the oligonucleotides were ordered on plates at 10, 100 or 250 nmole scales. UltraPure™ agarose-1000, SYBR Gold nucleic acid gel stain, FCF400-CU-50 TEM grids, boric acid, ethanol 200 proof, glycerol, 1.5 mm mini-gel cassettes, and SequaGel-UreaGel System were purchased from Thermo Fisher Scientific. Tris base (molecular biology grade), ethylenediaminetetraacetic acid (EDTA), disodium EDTA, magnesium chloride hexahydrate (MgCl_2 , 99.995 % and 99 %), sodium chloride (NaCl, 99 %), TLC silica gel 60G F254 glass plates, ammonium persulfate (APS), N,N,N',N'-tetramethyl ethylenediamine (TEMED), Tween 20, xylene cyanol FF, bromophenol blue and formamide (deionized) were ordered from Sigma-Aldrich. Uranyl formate was supplied by Electron Microscopy Sciences.

Buffer compositions

10× TEF buffer: 50 mM Tris base, and 10 mM EDTA acid (n.b. results in pH 8.0 at 25 °C when mixed at this ratio, without any need for further acid/base titration).

10× TBE buffer (1 L): 108 g Tris base, 55 g boric acid, and 5.84 g disodium EDTA.

Agarose gel loading buffer (AGLB): 30 % glycerol, 0.025 % xylene cyanol, 0.025 % bromophenol blue.

Formamide loading buffer (FLB, 50 mL): 47.5 mL deionized formamide, 12.5 mg bromophenol blue, 2.5 mg xylene cyanol FF, 500 μL 0.5 M EDTA solution (pH 8.0), and 2 mL Milli-Q water.

Milli-Q water was used throughout this study.

Experimental protocol

DNA-origami seed. The DNA-origami seed used in this study was designed and folded the same as our previous report.¹

DNA oligonucleotide sequence design. The architecture designs for branching growths were performed using scadnano,² and the sequences for corresponding DNA slats were assigned and optimized using custom Python scripts. All sequences were designed to have minimal self-structures and relatively isoenergetic binding sites assessed by NUPACK,^{3,4} while having a GC-content of ca. 50 % and avoiding any 6-nt repeats. Poly(thymidine) (polyT) brushes were added to the slats to prevent blunt-end-stacking induced ribbon aggregation.

DNA slats purification. All slats for crisscross assemblies were purified by denaturing polyacrylamide gel electrophoresis (dPAGE). Briefly, 15 wt.% dPAGE gels were prepared in empty 1.5 mm mini-gel cassettes using SequaGel UreaGel System. The plate oligonucleotides ordered at 10, 100, or 250 nmole scale were rehydrated with 50 μ L (for 10 nmole plates) or 100 μ L (for 100 or 250 nmole plates) of Milli-Q water. Unless otherwise mentioned, the oligonucleotides were combined into pools, e.g., pools for nuc-y-slats, x-slats, branching nuc-y-slats, branching x-slats, branching y-slats, etc. The pools were mixed with equivalent volume of FLB. Samples were then loaded onto the dPAGE gel, with ca. 2–3 nmole per lane, followed by running the gel at 300 V for ca. 1 h in 0.5 \times TBE buffer, usually until the bromophenol blue dyes had run off the gel. Afterwards, the gel was wrapped in cling film and then placed on the TCL plate. The gel bands were identified by shadowing with UV light, marked using a marker pen, and then excised with a razor blade. An individual gel slice (no more than two lanes) was placed into a 2 mL round-bottom Eppendorf tube and crushed using a pestle, followed by adding 500 μ L 1 \times TEF buffer. After shaking overnight at 37°C and 1500 rpm, the mixture was transferred to a Freeze N' Squeeze spin column (Bio-Rad) and spun at 10k rpm for 15–20 minutes. The filter containing waste acrylamide was then discarded, and 3 volumes of 100 % ethanol that had been pre-cooled at -20°C, along with 1/10 volume of 3 M NaCl, were then added to the Freeze N' Squeeze tube. The tube was then inverted several times to ensure thorough mixing of the contents. Afterwards, the tubes of different pools were placed into a pre-cooled centrifuge (at ca. -9 °C), and spun at 20k rcf for 30 min, followed by removing the supernatant. The resulting pellets were washed twice with 75 % ethanol using the centrifuge, with each spin lasting 15 minutes. The pellets were then dried at room temperature for ca. 20 mins, followed by rehydrating with 15–20 μ L Milli-Q water. The concentration was then determined by a Nanodrop 2000c UV-Vis spectrophotometer. The final working stocks were prepared at a concentration of 5 or 10 μ M for each slat.

Agarose gel electrophoresis (AGE). 0.5 wt.% agarose gel was prepared in 0.5× TBE buffer containing 12 mM MgCl₂ with a volume of ca. 160 mL, which was pre-stained with 3 or 6 μL SYBR gold (10,000× concentrate in DMSO) after the molten agarose was cooled to ca. 65 °C. Usually, 3 μL each reaction mixture was taken and mixed with 5 μL AGLB, and the mixed samples were then loaded onto the agarose gel. During the preparation and running processes of AGEs, dye bleaching was minimized by covering the gels with aluminum foil. All the agarose gels in this study were run at 65 V for 2–3 h in 0.5× TBE buffer containing 12 mM MgCl₂, followed by recording using a GE Typhoon FLA 9500 fluorescent imager. The obtained pictures were then proceeded with ImageJ (v2.0.0-rc-69/1.52i).

TEM analysis. The structures were visualized through TEM by applying a negative stain to the samples. TEM grids were first cleaned using plasma discharge for 25 s, followed by placing 4 μL of the reaction mixture to the grid (for samples from linear growth, a 10-fold dilution was applied). After 2 min, the solution was wicked from the grid by gently touching filter paper to the grid edge. 4 μL of uranyl formate solution (2 % w/v in H₂O, filtered through a 0.22 μm pore size membrane) was then placed onto the grid and the excess solution was immediately wicked using filter paper. The images were captured on a JEOL JEM-1400Plus TEM in brightfield mode at 80 kV.

Crisscross polymerization of ssDNA slats. Unless otherwise mentioned, all the reactions were carried out at a total volume of 10 μL. For a typical linear growth reaction, the experiment was conducted in 1× TEF buffer containing 1 nM DNA-origami seed, 0.5 μM each nuc-y slat, x-slat, and y-slat, 16 mM MgCl₂, 0.01 % Tween 20. The reaction mixture, without the origami seed, was first denatured at 85 °C for 5 min, after which the temperature was maintained constant at 48 °C, followed by adding 1 μL of 10 nM origami seed to start the growth. The growth time varies from 1 to 16 h. Afterwards, the obtained ribbons were characterized by AGE and TEM. To identify the optimal conditions for growth, we conducted growth experiments under varying temperature and MgCl₂ concentration.

Sequence screening for linear growth. Five sequence variants were generated using Python script (v6.0–v6.4). The slats were pooled and purified by dPAGE as described above. The experiments were conducted in 1× TEF buffer containing 1 nM DNA-origami seed, 0.5 μM each nuc-y slat, x-slat, and y-slat, 14 mM MgCl₂, 0.01 % Tween 20. The reaction mixture without seed was first denatured at 85 °C for 5 min, after which the temperature was maintained constant at 46 °C, followed by adding 1 μL of 10 nM seed to start the growth. For the spurious control experiments, 1 μL buffer (1× TEF supplemented with 6 mM MgCl₂) was added, instead of the seed. After reacting at 46 °C for ca. 16 h, the growths were analyzed using AGE.

Screening optimal growth conditions. The experiments were carried out using v6.0 sequences. We first checked the growths at varied concentrations of MgCl₂. The experiments were conducted in 1× TEF buffer

containing 1 nM DNA-origami seed, 0.5 μ M each nuc-y slat, x-slat, and y-slat, 12, 14, 16 or 18 mM $MgCl_2$, and 0.01 % Tween 20. The reaction mixtures, without the DNA-origami seed, were first denatured at 85 °C for 5 min, after which the temperature was maintained constant at 48 °C, followed by adding 1 μ L of 10 nM seed and growing for 16 h. Afterwards, 3 μ L of the reaction mixture was taken from each reaction and mixed with 5 μ L of AGLB containing 12 mM $MgCl_2$. The prepared samples were then analyzed by AGE as described above.

To further test the optimal temperature for the growth, the experiments were carried out at 46, 48, 50 and 52 °C by using 14 or 16 mM $MgCl_2$, with the other conditions the same as above.

Ribbon growths at varied slat concentrations. The experiments were carried out in 1 \times TEF buffer containing 1 nM DNA-origami seed, 0.5, 1 or 2 μ M each slat, 16 mM $MgCl_2$, 0.01 % Tween 20. The reaction mixtures, without the DNA-origami seed, were first denatured at 85 °C for 5 min, after which the temperature was maintained constant at 48 °C, followed by adding 1 μ L of 10 nM seed and growing for 16 h. Afterwards, 3 μ L of the reaction mixture was taken from each reaction and mixed with 5 μ L of AGLB containing 12 mM $MgCl_2$. The prepared samples were then analyzed by AGE as described above. The lengths of the assembled ribbons were characterized by TEM and quantified using ImageJ.

Extension optimization. Three sequence variants of each x-extension were designed on the v6.0 core sequences. All the x-slats, without or with the six-segments x-extension, were individually purified using dPAGE. In the first-round x-extensions screening, the extensions on the first three and last three x-slats were independently screened, with $3 \times 3 \times 3 = 27$ different combinations for each set of three extensions. The experiments were carried out in 1 \times TEF buffer containing 1 nM origami seed, 0.5 μ M each nuc-y slat, x-slat, and y-slat, 16 mM $MgCl_2$, 0.01 % Tween 20. The reaction mixtures, without the DNA-origami seed, were first denatured at 85 °C for 5 min, after which the temperature was maintained constant at 48 °C, followed by adding 1 μ L of 10 nM seed and growing for 16 h. Afterwards, 3 μ L of the reaction mixture was taken from each reaction and mixed with 5 μ L of AGLB containing 12 mM $MgCl_2$. The prepared samples were then analyzed by AGE the same as above. For the second-round x-extensions screening, the extension combinations showing good performances from both groups were further used to create new combinations for screening all six x-extensions in a single reaction, and the experiments were conducted the same as above.

Primary branching (PriB) growth with a growth direction perpendicular to the core ribbon. The experiments were conducted in 1 \times TEF buffer containing 0.3 nM DNA-origami seed, 0.5 μ M each nuc-y slat, x-slat, y-slat, branching nuc-y slat, branching x-slat, and branching y-slat, 16 mM $MgCl_2$, 0.01 % Tween 20. The reaction mixtures, without the DNA-origami seed, were first denatured at 85 °C for 5 min, after

which the temperature was maintained constant at 48 °C, followed by adding 1 µL of 3 nM seed and growing for 1 h. Afterwards, 3 µL of the reaction mixture was taken from each reaction and mixed with 5 µL of AGLB containing 12 mM MgCl₂. The prepared samples were then analyzed by AGE the same as above. Additionally, the growths using 10 pM seed were performed the same as above and had a growth time of 14 h.

PriB growth with a growth direction opposite to the core ribbon growth. The experiments were conducted in 1× TEF buffer containing 0.1 nM DNA-origami seed, 0.5 µM each nuc-y slat, x-slat, y-slat, branching nuc-y slat, branching x-slat, and branching y-slat, 16 mM MgCl₂, 0.01 % Tween 20. The reaction mixtures, without the DNA-origami seed, were first denatured at 85 °C for 5 min, after which the temperature was maintained constant at 48 °C, followed by adding 1 µL of 1 nM seed and growing for 1 and 19 h. Afterwards, 3 µL of the reaction mixture was taken from each reaction and mixed with 5 µL of AGLB containing 12 mM MgCl₂. The prepared samples were then analyzed by AGE the same as above. The morphologies for the structures were further characterized by TEM.

Furthermore, the growths were carried out using 1 pM seed, and the concentration of each slat was increased from 0.5 to 1 µM, while the other conditions maintained the same.

Extension optimization for secondary branching (SecB) growth. The process for the extension optimization followed with the same process as above, except that y-extensions were added to the ribbon and v6.4 sequences were used as the core ribbon. After the y-extensions optimization, the v6.4 sequences with y-extensions were plugged to the v6.0 sequences with x-extensions, so that v6.3 sequences can be further used for the SecB growth off the y-extensions on primary branches (v6.4 sequences).

SecB growth. The experiments were conducted in 1× TEF buffer containing 1 pM DNA-origami seed, 0.2 µM each nuc-y slat, 0.2 µM each core slat, 0.25 µM each PriB growth slat, 0.5 µM each SecB growth slat, 16 mM MgCl₂, and 0.01 % Tween 20. The reaction mixtures, without the DNA-origami seed, were first denatured at 85 °C for 5 min, after which the temperature was maintained constant at 48 °C, followed by adding 1 µL of 10 pM seed and growing for 4 and 12 h. Afterwards, 3 µL of the reaction mixture was taken from each reaction and mixed with 5 µL of AGLB containing 12 mM MgCl₂. The prepared samples were then analyzed by AGE the same as above. The morphologies for the structures were further assessed by TEM.

Furthermore, to tune the morphology of the final structures, the experiments were also conducted using 0.5 µM of each slat, while the other conditions were maintained the same.

Hyperbranching (HypB) growth. The experiments were conducted in 1× TEF buffer containing 10 fM DNA-origami seed, 0.2 µM each nuc-y slat, 0.5 µM core slat, 0.25 µM each branching nuc-y and adapter slat,

16 mM MgCl₂, and 0.01 % Tween 20. The reaction mixtures, without the origami seed, were first denatured at 85 °C for 5 min, after which the temperature was maintained constant at 50 °C, followed by adding 1 µL of 0.1 pM seed. At different time intervals (0.5, 1, 2 and 4 h), samples were collected and characterized using TEM.

Limit of detection (LoD) using p8064. The experiments were performed with the same conditions as the HypB growth above, except that varied concentrations of the target strand were used (from 1 pM to 100 aM with one order of magnitude decrease per reaction), and 0.2 µM each nuc-x slat, instead of nuc-y slat, was used. After reacting for 1 or 4 h, 3 µL of the reaction mixture was taken from each reaction and mixed with 5 µL of AGLB containing 12 mM MgCl₂. The prepared samples were then analyzed by AGE the same as above.

LoD using a synthetic ultramer target. For the experiments with a target concentration from 1 pM to 100 aM target, the experiments were conducted in 1× TEF buffer containing 0.1 µM each nuc-x slat, 0.25 each short pre-y slat, 0.5 µM core slat, 0.25 µM each branching nuc-y slat and adapter slat, 16 mM MgCl₂, and 0.01 % Tween 20, with a final reaction volume of 10 µL. After adding all the components together, the reaction mixtures were denatured at 85 °C for 5 min, followed by incubating at 50 °C for 4 h. Afterwards, 3 µL of the reaction mixture was taken from each reaction and mixed with 5 µL of AGLB containing 12 mM MgCl₂. The prepared samples were then analyzed by AGE the same as above.

The experiments with a target concentration from 1 fM to 100 zM were conducted at a final reaction volume of 20 µL, containing 0.1 µM each nuc-x slat, 0.125 µM each short pre-y slat, 0.25 µM each core slat, 0.125 µM each branching nuc-y slat and adapter slat, 16 mM MgCl₂, and 0.01 % Tween 20. After adding all the components together, the reaction mixtures were denatured at 85 °C for 5 min, followed by incubating at 50 °C for 16 h. Afterwards, 10 µL of AGLB containing 12 mM MgCl₂ was added into each reaction mixture. The prepared samples were then analyzed by AGE the same as above.

Amplification of targets diluted to small numbers per well. The ultramer target solution was dilute to a concentration of 10 aM in 1× TEF buffer containing 6 mM MgCl₂, for which there are ca. 6 copies per µL. Then, the desired nominal number of copies (i.e. based on the mean number of copies expected for that volume, usually 2–12 copies; the actual number of copies is expected to vary according to a Poisson distribution from volume to volume) was taken and split into multiple reactions for HypB growths. For instance, to split 3 nominal copies into 10 reactions, 0.5 µL of the 10 aM solution was taken and diluted to 9.5 µL 1× TEF buffer containing 6 mM MgCl₂, followed by splitting the 10 µL mixture into ten PCR tubes, with 1 µL for each. Afterwards, 9 µL solution containing all the assembling slats for HypB growth was added to each tube, leading to a final volume of 10 µL, with 1× TEF, 16 mM MgCl₂, 0.1 µM each nuc-x slat,

0.125 μM each short pre-y slat, 0.25 μM each core slat, and 0.125 μM each branching nuc-y slat and adapter slat. Then, the reaction mixtures were denatured at 85 $^{\circ}\text{C}$ for 5 min, followed by incubating at 50 $^{\circ}\text{C}$ for ca. 16 h. Afterwards, 10 μL AGLB was added into each tube, and the prepared samples were then analyzed by AGE the same as above.

Calculation of second-order rate constant. The length of the ribbons measured from TEM images was used to approximate the second-order rate constant for linear growths. The second-order rate constant was estimated with: $\tau = t_{1/2}/\ln(2) = 1/(kC_0)$, where the τ is the mean dwell time, $t_{1/2}$ is the half-life, C_0 is the initial DNA slat concentration, and k is the second-order rate constant.¹ Note: the addition of each x- or y-slat is estimated to increase the ribbon length by 1.5 nm.

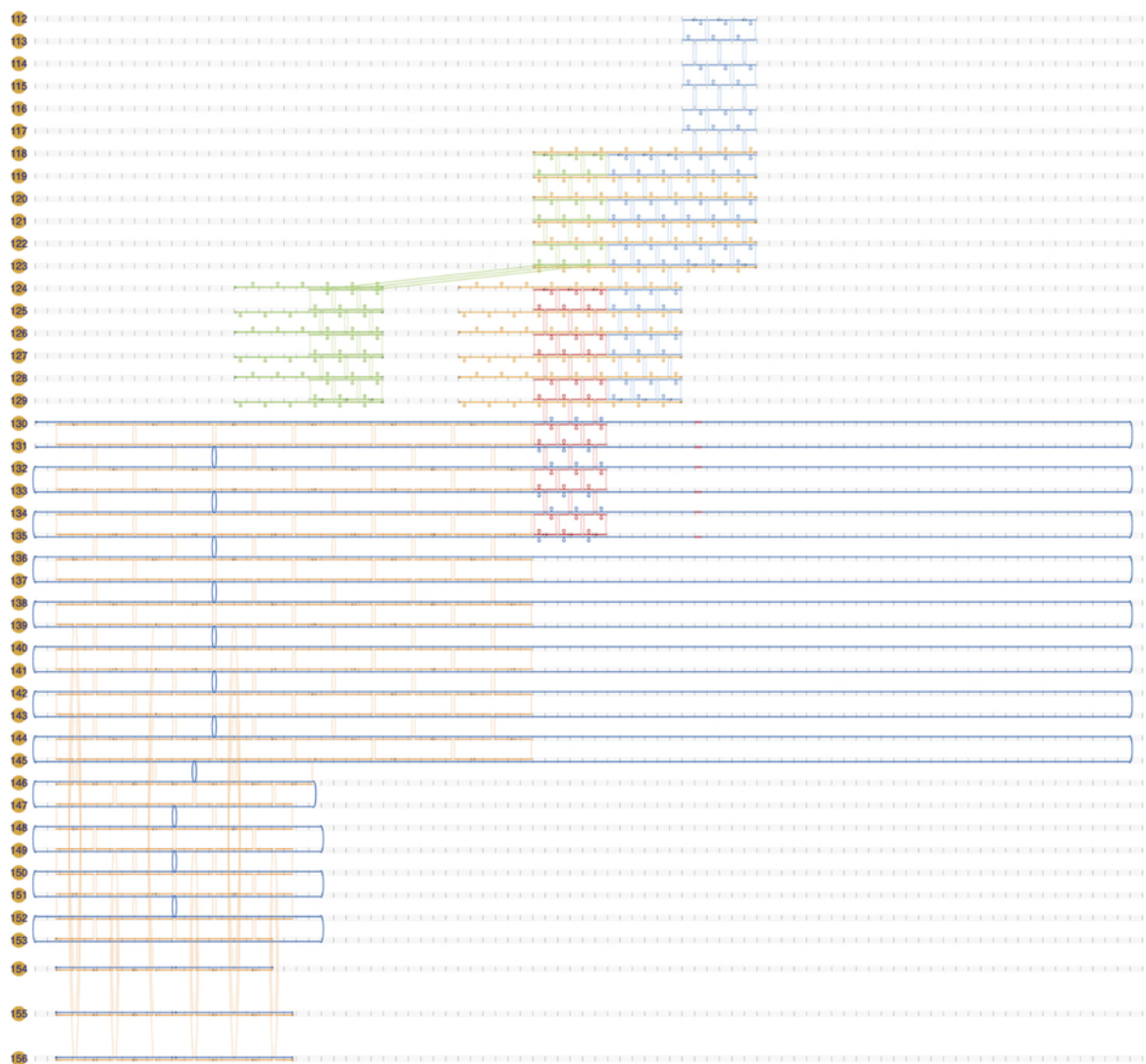


Figure S1. Strand rooting diagram for HypB growth off a DNA-origami seed.

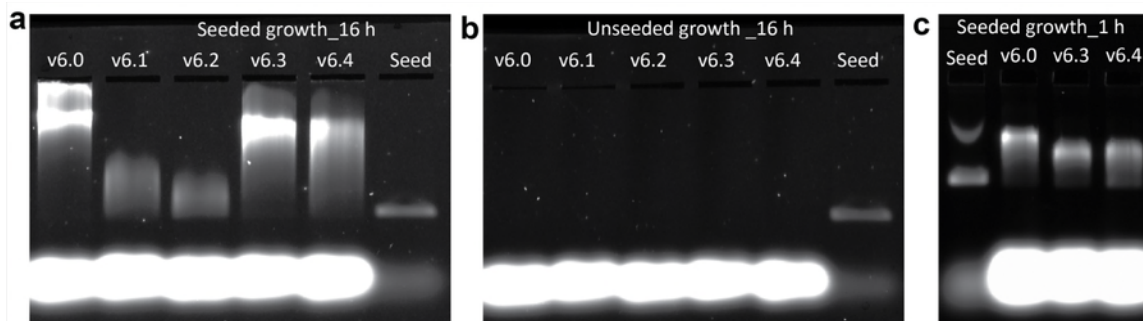


Figure S2. Sequence screening for linear zigzag ribbon growth. a–b) AGE analyses of **(a)** seeded and **(b)** unseeded crisscross polymerization of five sequence variants. **c)** AGE analyses of crisscross polymerization of v6.0, v6.3 and v6.4 ribbons for a growth time of 1 h. This indicates that v6.0 has the best performance. Conditions: **a)** 1× TEF buffer with 14 mM MgCl₂, 1 nM DNA-origami seed, 0.5 μM each assembling slat, and 46 °C for 16 h. **c)** The same as **a)** but used 16 mM MgCl₂ and incubated at 48 °C for 1 h.

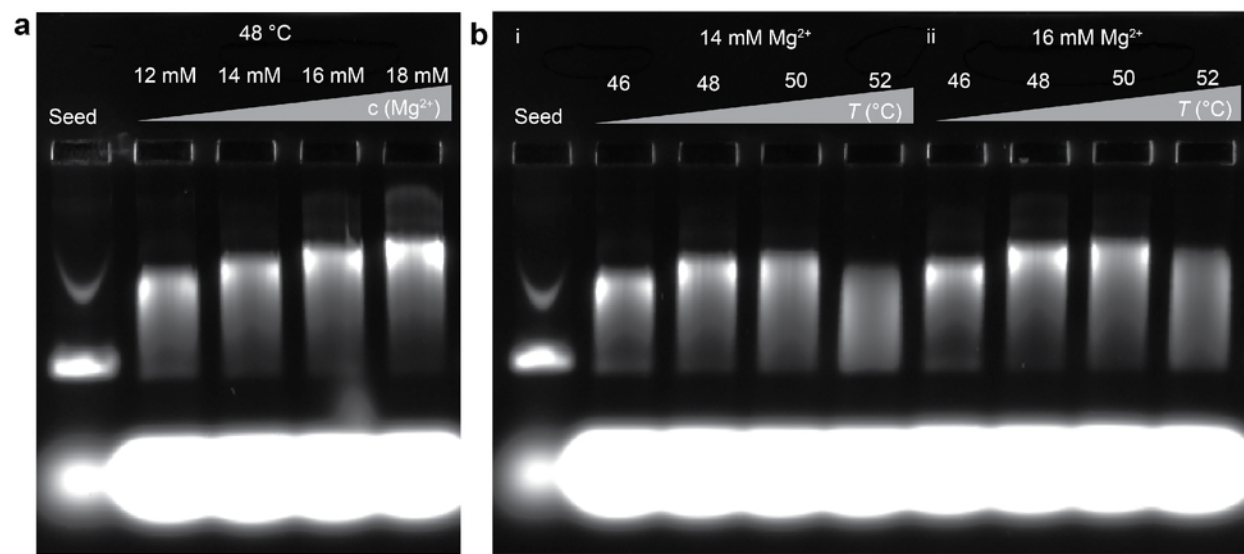


Figure S3. Screening optimal growth conditions. a) AGE analyses of crisscross polymerization of v6.0 ribbon at varied magnesium concentrations. b) AGE analyses of crisscross polymerization of v6.0 ribbon at varied temperatures using (i) 14 and (ii) 16 mM $MgCl_2$. Conditions: 1× TEF buffer, 1 nM DNA-origami seed, and 0.5 μ M each slat.

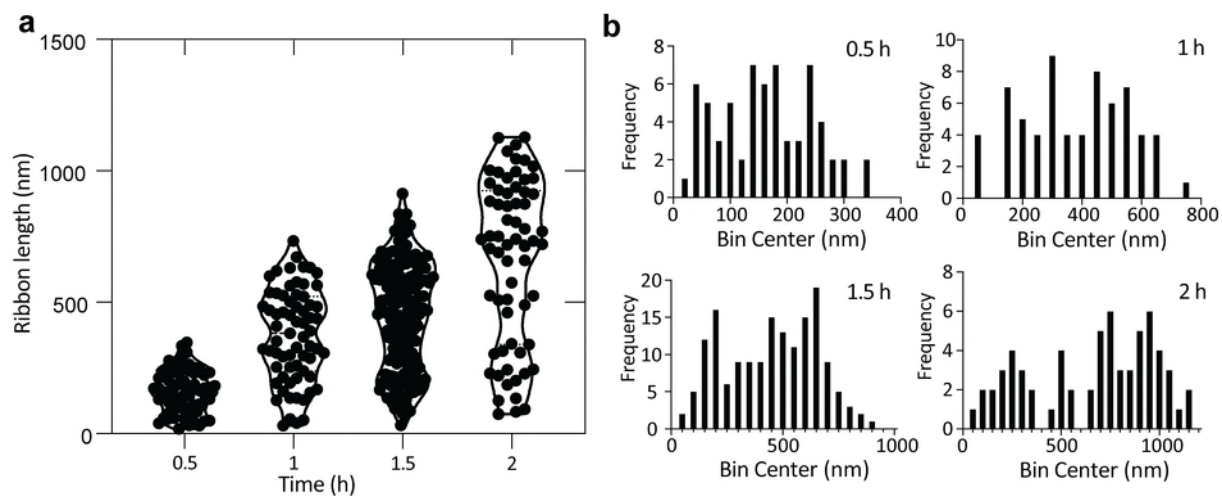


Figure S4. Ribbon length distribution for linear growth using 0.5 μ M each slat. a) violin and b) histogram plots for lengths of ribbons without x-extensions as a function of time.

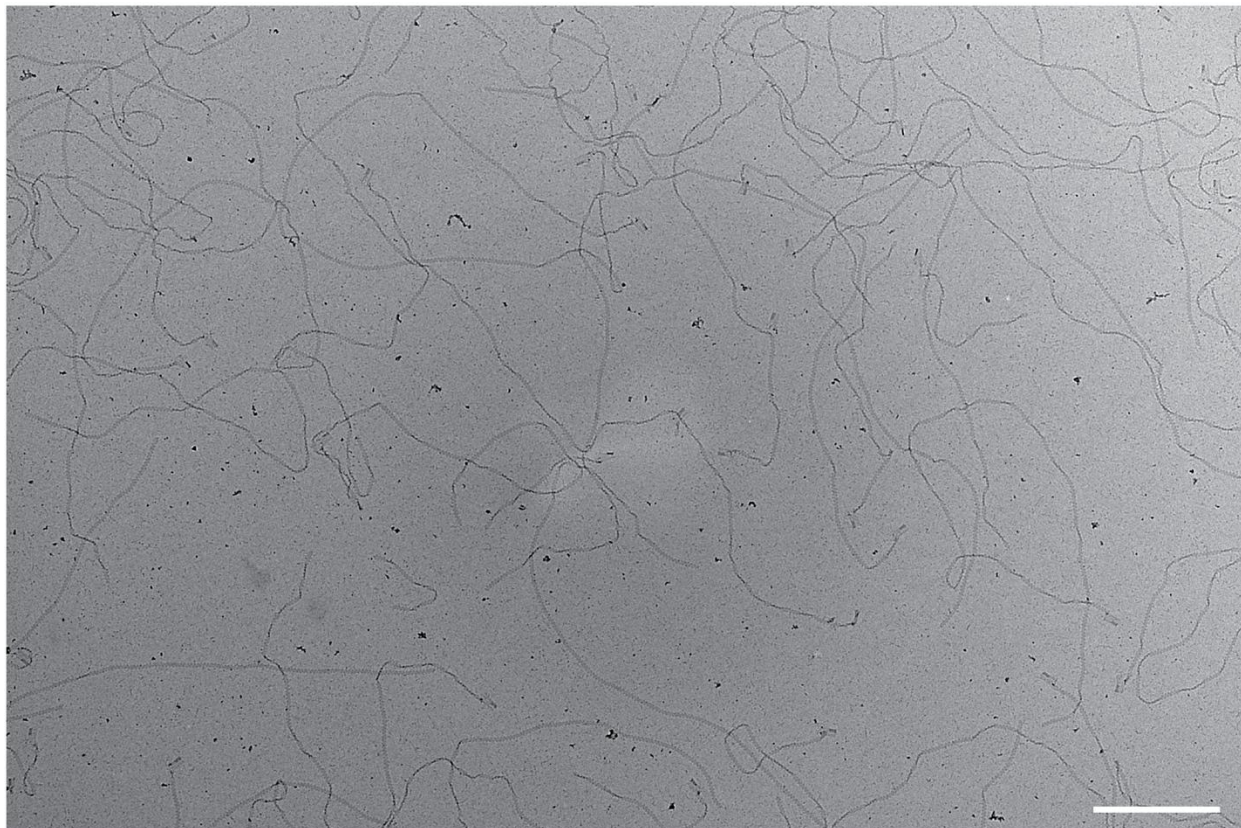


Figure S5. Crisscross polymerization of v6.0 ribbon. TEM image of the ribbons after growing at 48 °C for 16 h. Scale bar: 600 nm. Conditions: 1× TEF buffer, 16 mM MgCl_2 , 1 nM origami seed, and 0.5 μM each slat.

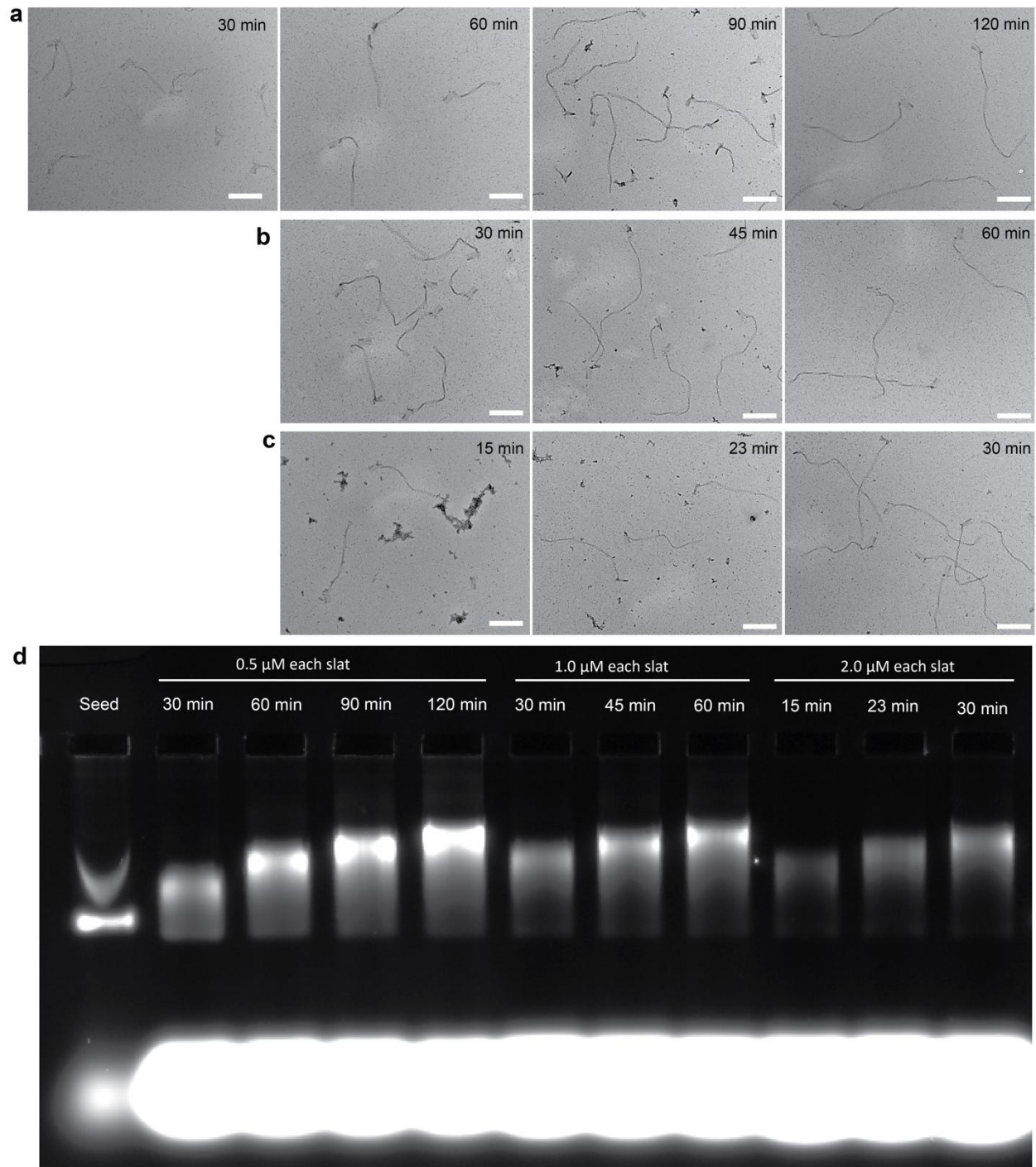


Figure S6. Ribbon growths at varying slat concentrations. a–c) Time-dependent TEM images of v6.0 ribbons growing at (a) 0.5 μM each slat, (b) 1 μM each slat, and (c) 2 μM each slat. d) AGE analyses of v6.0 ribbon growths at varying slat concentrations. Scale bars: 200 nm. Conditions: 48 $^{\circ}\text{C}$, 1 \times TEF buffer, 16 mM MgCl_2 , and 1 nM DNA-origami seed.

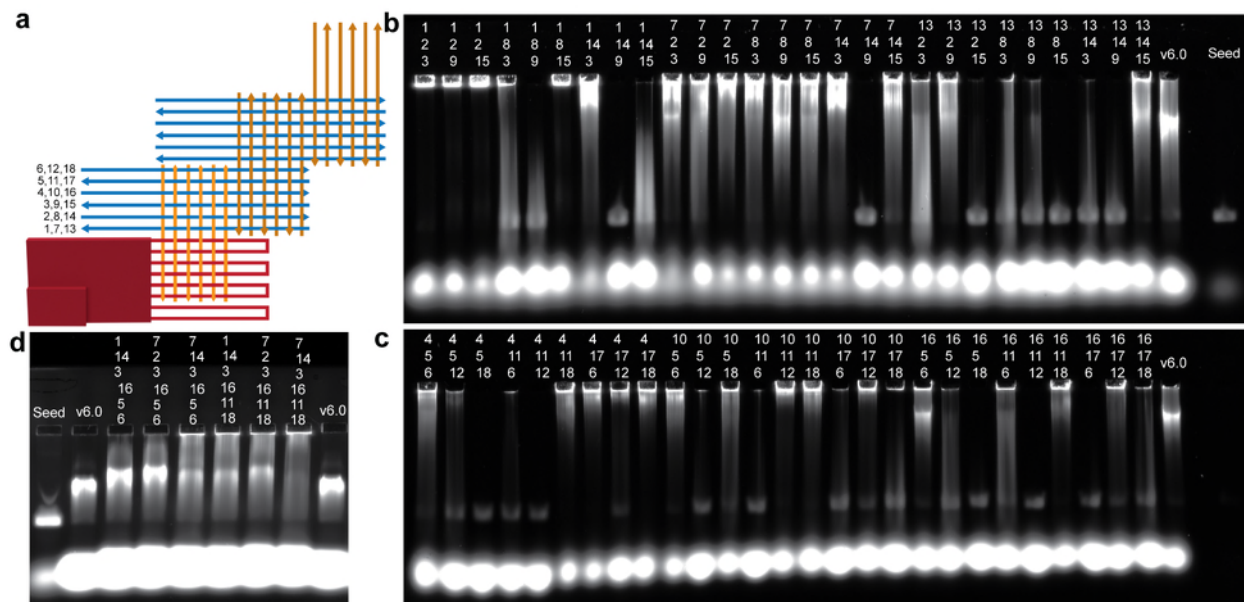


Figure S7. Extensions optimization for v6.0 ribbon. **a)** Schematic illustration of linear ribbon growth with six x-extensions. The numbers next to the extensions represent numbered sequence variants for the extensions. **b)** AGE analyses of the ribbon growths with the first three x-extensions. **c)** AGE analyses of the ribbon growths with the second three x-extensions. **d)** AGE analyses of the ribbon growths with all six x-extensions. Conditions: 48 °C, 1× TEF buffer, 16 mM MgCl₂, 1 nM DNA-origami seed, and 0.5 μM each slat. Note: the combination of extensions numbered 1, 14, 3, 16, 5, and 6 was further used for the branching growths.

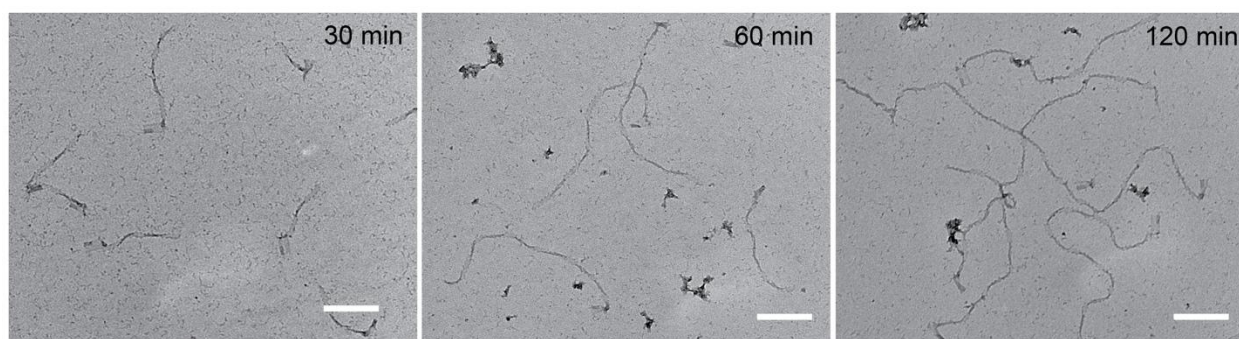


Figure S8. Crisscross polymerization of v6.0 ribbons with six-segments x-extensions. Time-dependent TEM images for the ribbon growths. Scale bars: 200 nm.

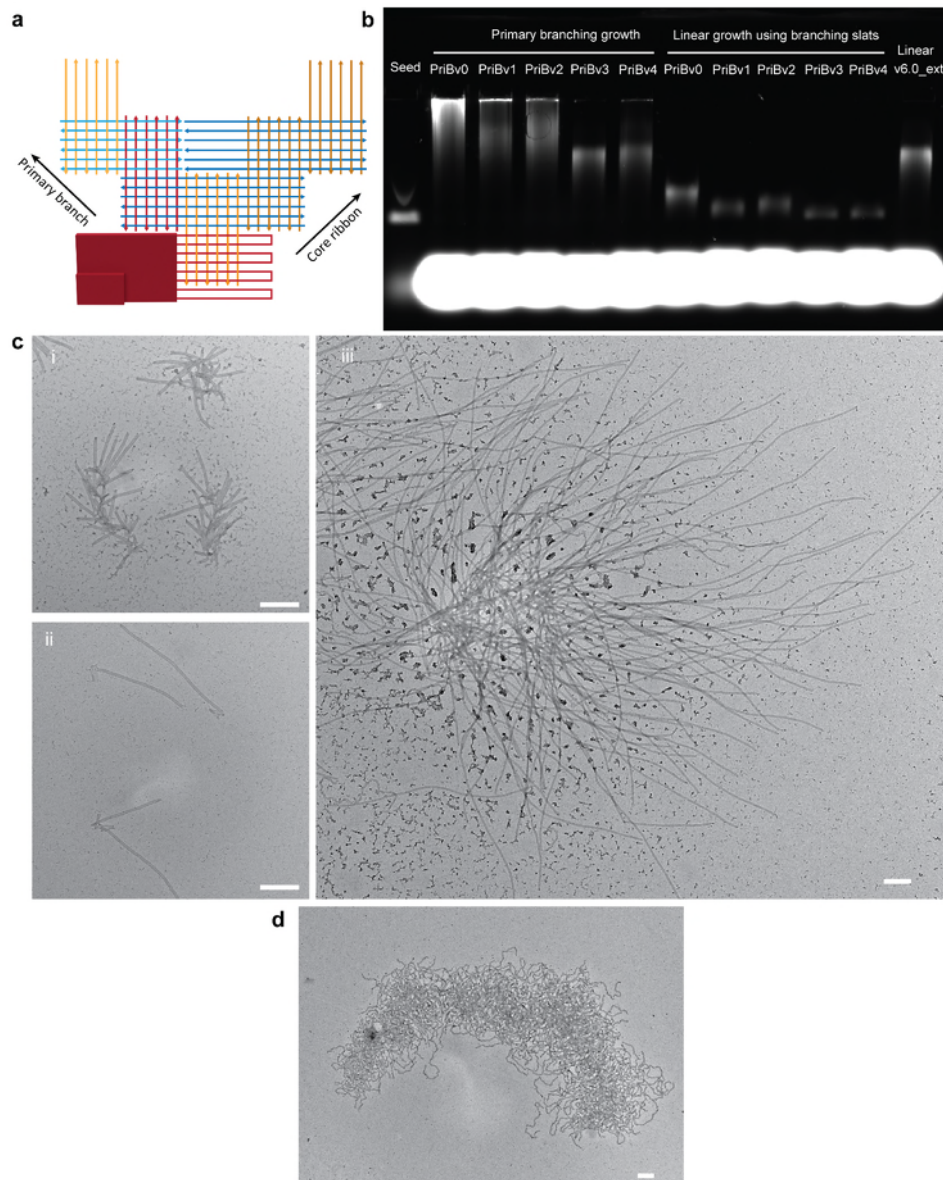


Figure S9. Primary branching (PriB) growth with a growth direction perpendicular to the core ribbon. **a)** Schematic illustration of PriB growth. **b)** AGE analyses of PriB growths and linear growths towards the northwest. Five sequences variants were tested. **c)** TEM images for (i) PriB growth with a growth time of 1h, (ii) linear growth towards the northwest with a growth time of 1 h, and (iii) PriB growth with a growth time of 14 h. **d)** TEM image for PriB growth with a growth time of 18 h, for which there are 7-nt T brushes on both sides of the branching x slats. Scale bars: 200 nm. Conditions: 48 °C, 0.3 nM DNA-origami seed, 0.5 μ M each slat, 16 mM MgCl_2 . 0.01 nM seed was used for c-iii.

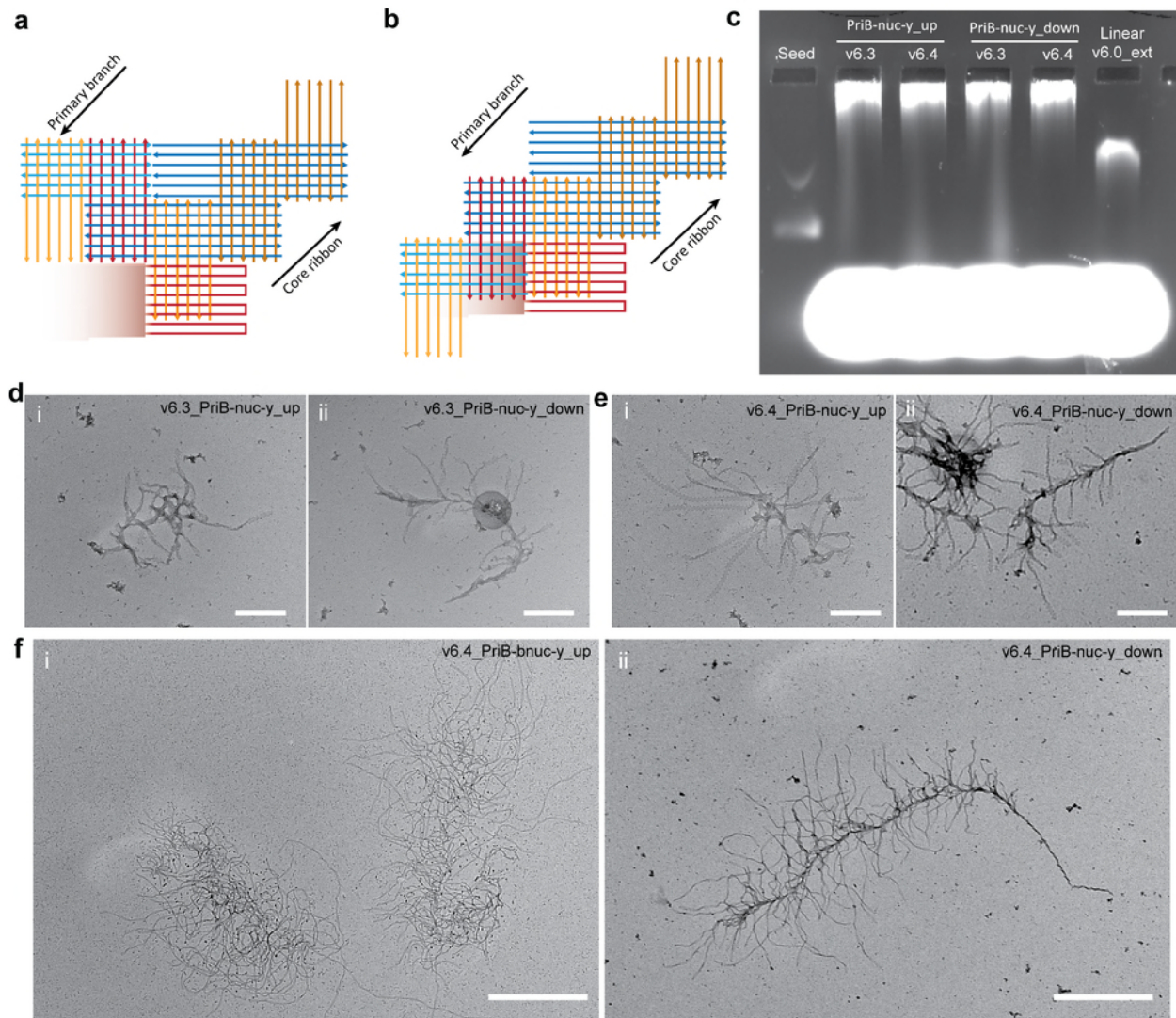


Figure S10. PriB growth with a growth direction opposite to the core ribbon. a–b) Schematic illustrations for PriB growths with the branching nuc-y slats pointing (a) up and (b) down. **c)** AGE analyses of PriB growths with a growth time of 1 h, using v6.0 sequences as the core ribbon and v6.3 or v6.4 sequences as the primary branches. **d)** TEM images for PriB growths with a growth time of 1 h using v6.3 sequences for the primary branches, with the branching nuc-y slats pointing (i) up and (ii) down. **e)** TEM images for PriB growths with a growth time of 1 h using v6.4 sequences for the primary branches, with the branching nuc-y slats pointing (i) up and (ii) down. **f)** TEM images for PriB growths with a growth time of 19 h using v6.4 sequences for the primary branches, with the branching nuc-y slats pointing (i) up and (ii) down. Scale bars: (d,e) 200 nm and (f) 800 nm. Conditions: 48 °C, 0.1 nM seed, 0.5 μ M each slat, and 16 mM MgCl_2 .

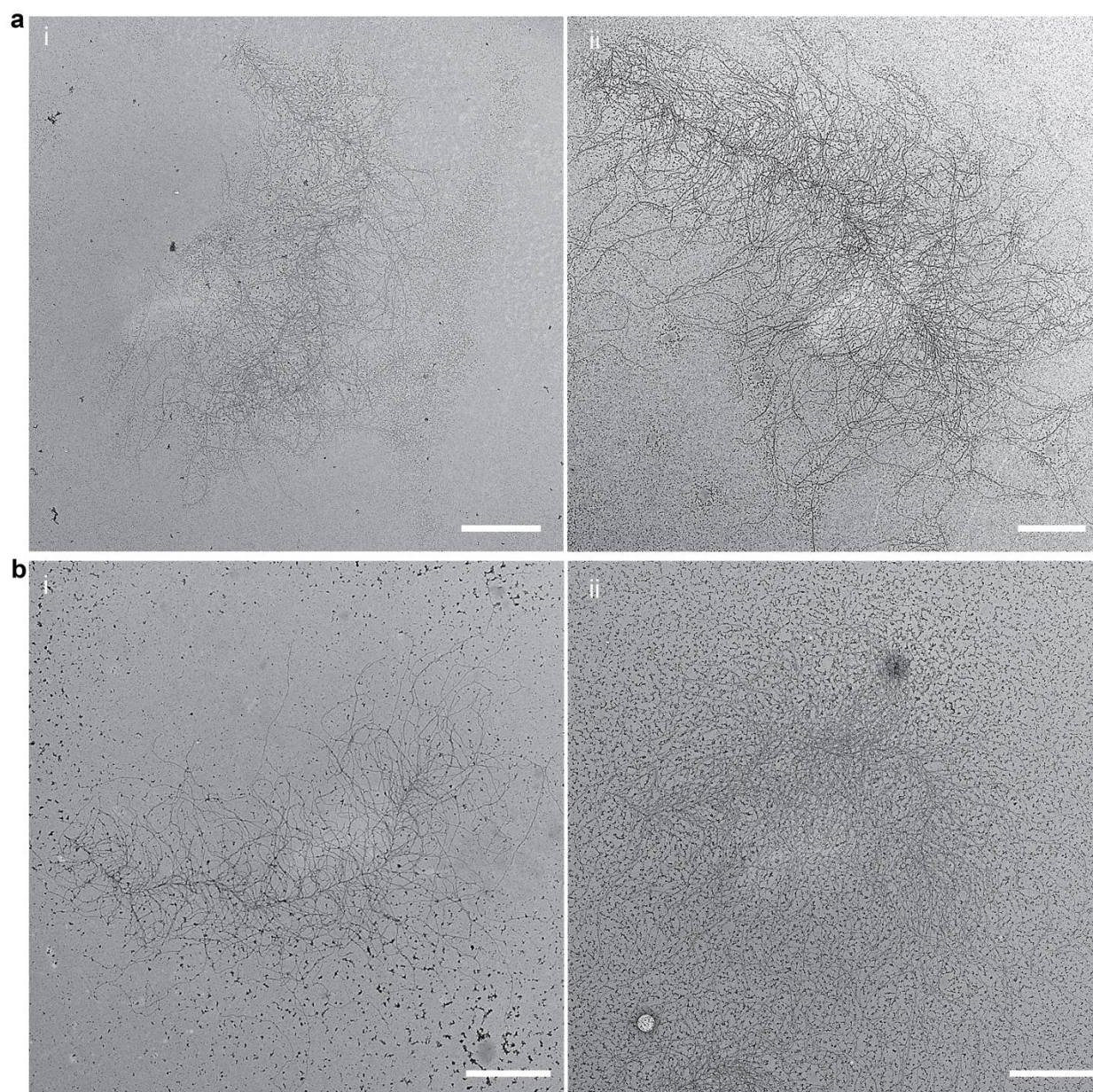


Figure S11. PriB growths with varied concentrations of branching slats. **a)** TEM images of PriB growths with v6.3 branches, using (i) 0.5 and (ii) 1 μM each branching growth slat. **b)** TEM images of PriB growths with v6.4 branches, using (i) 0.5 and (ii) 1 μM each branching growth slat. Scale bars: 1 μm . Conditions: 10 pM seed, 0.5 μM each core slat, 16 mM MgCl_2 , 48 $^\circ\text{C}$, and 16 h.

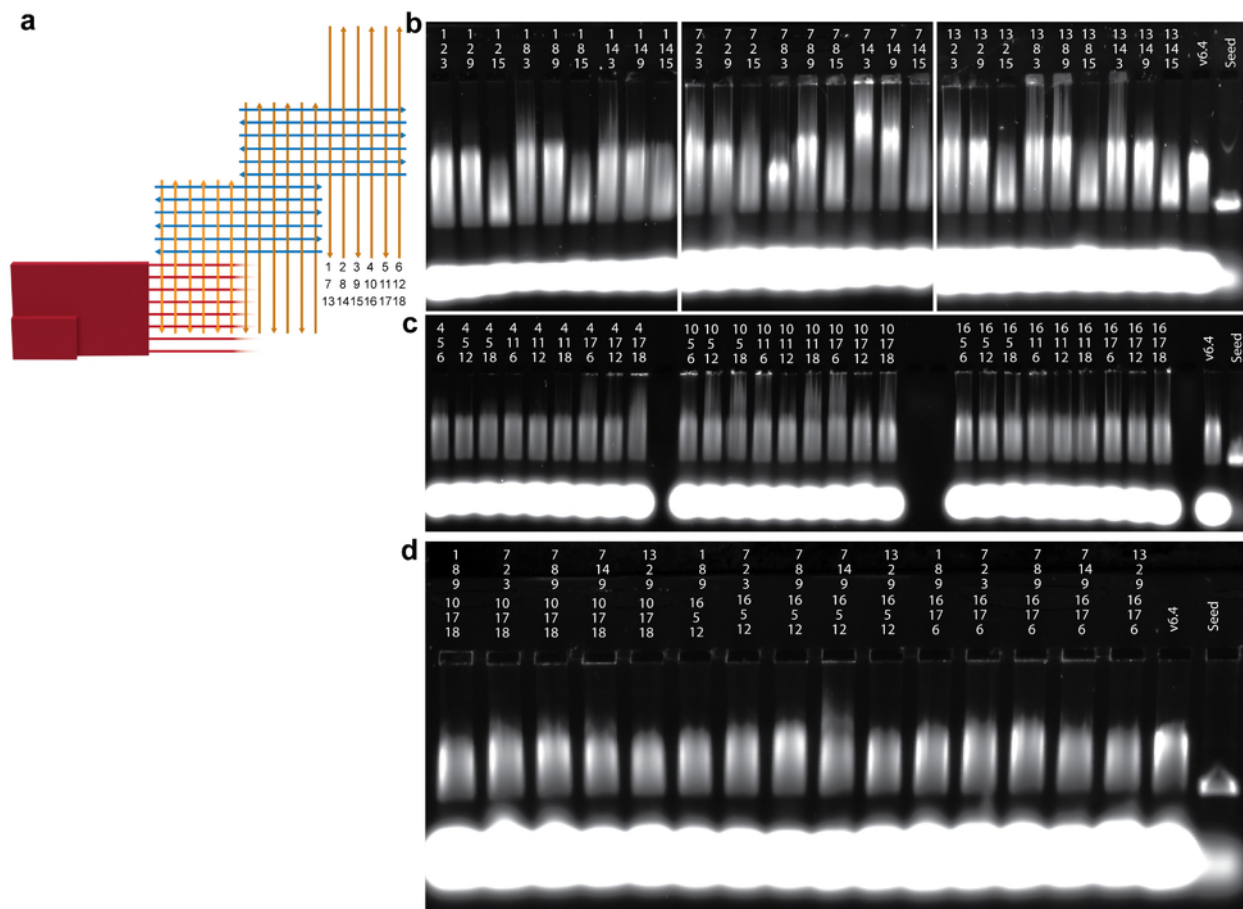


Figure S12. Sequence optimization for the six-segments y-extensions. **a)** Schematic illustration for the zigzag ribbon with six y-extensions. The numbers next to the extensions represent numbered sequence variants for the extensions. **b)** AGE analyses of the ribbon growths with the first three six-segments y-extensions. **c)** AGE analyses of the ribbon growths with the second three six-segments y-extensions. **d)** AGE analyses of the ribbon growths with all six y-extensions. Conditions: 48 °C, 1× TEF buffer, 16 mM MgCl₂, 1 nM DNA-origami seed, 0.5 μM each nuc-y slat, x-slat, and y-slat, and a growth time of 3 h. Note: the combination of extensions numbered 7, 8, 9, 16, 17, and 6 was further used for secondary branching growth.

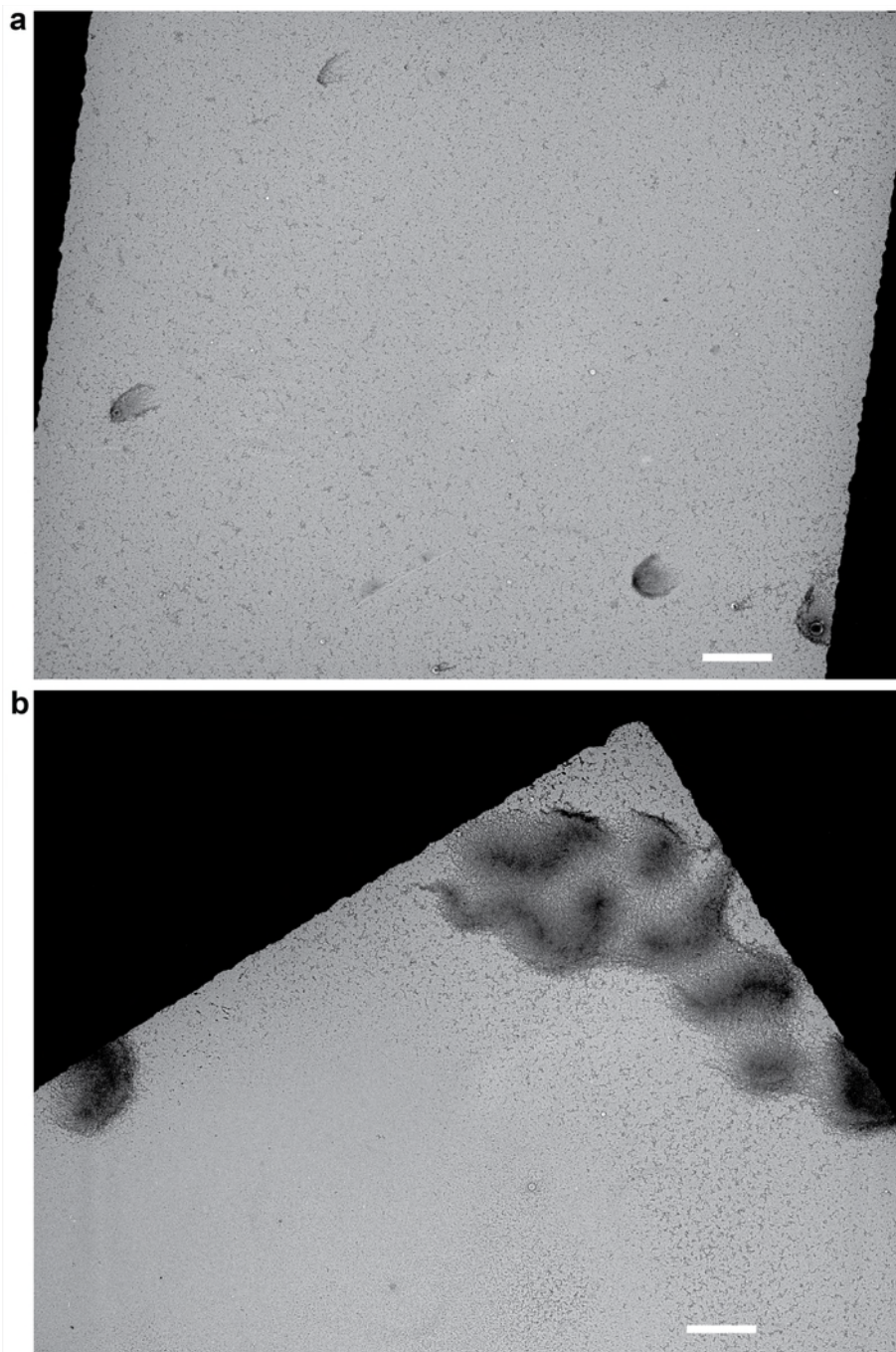
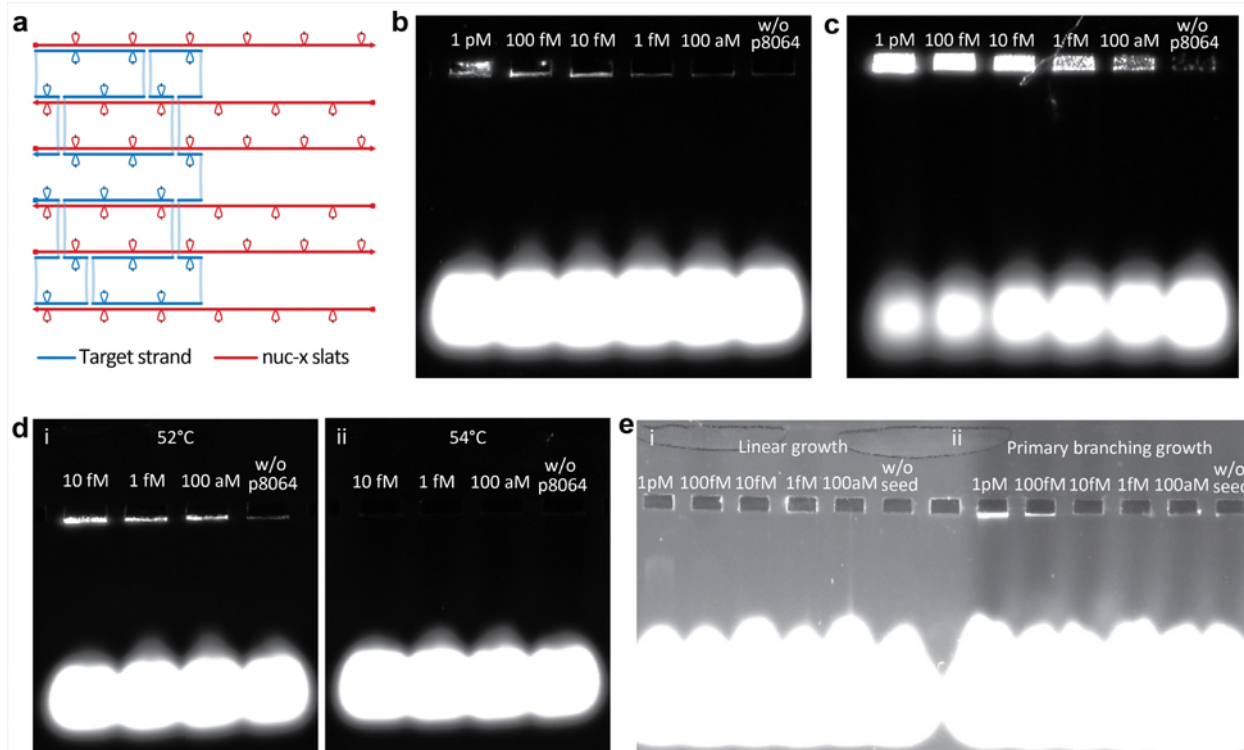


Figure S13. Secondary branching (SecB) growth. a–b) Zoomed-out TEM images of SecB growths with a growth time of (a) 4 and (b) 12 h. Scale bars: 3 μm . Conditions: 48°C, 1 pM seed, 0.5 μM each periodic slat, 0.2 μM each nuc-y slat, and 16 mM MgCl_2 .



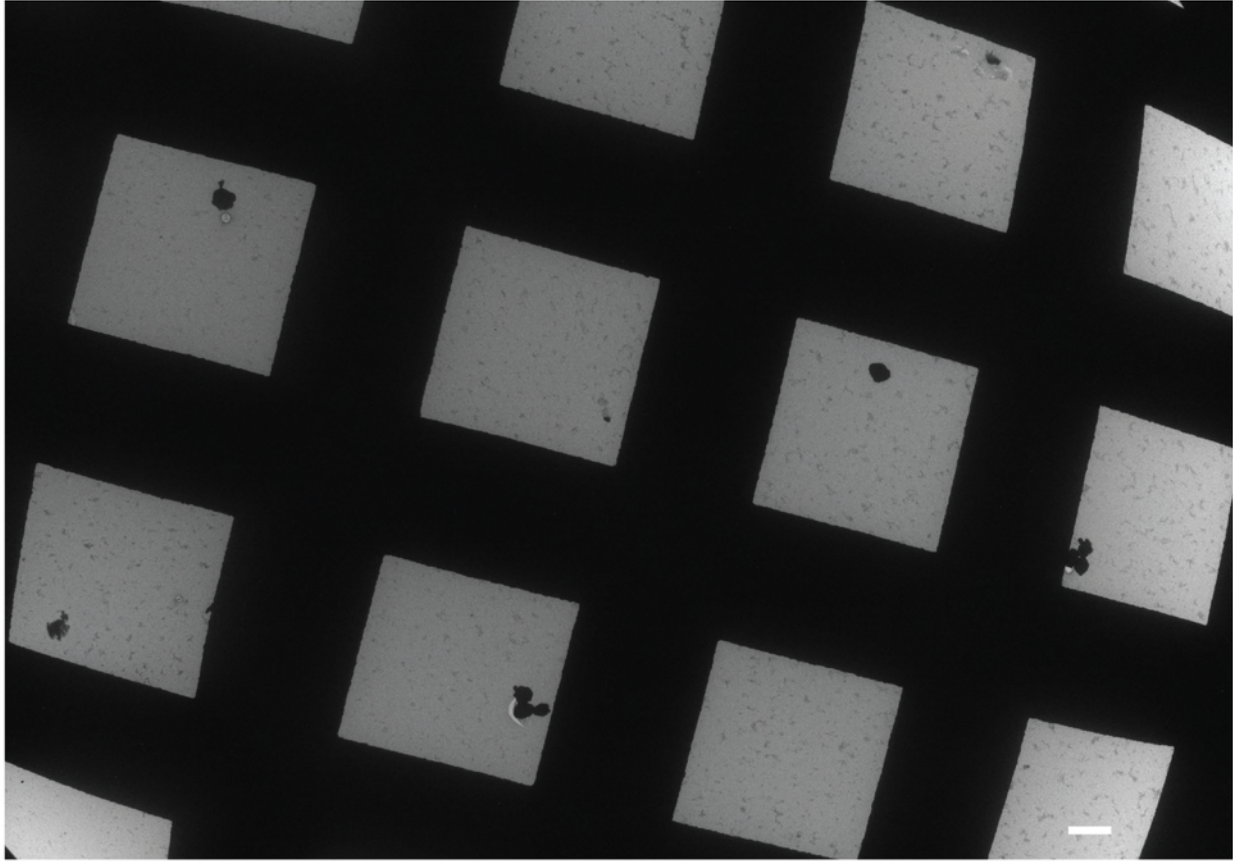


Figure S15. HypB growth. Zoomed-out TEM image of HypB growth with a growth time of 4 h. Scale bar: 10 μm . Conditions: 50 °C, 16 mM MgCl_2 , 10 fM seed, 0.2 μM each nuc-x slat, 0.5 μM each core ribbon growth slat, and 0.25 μM each branching nuc-y slat and adapter slat.

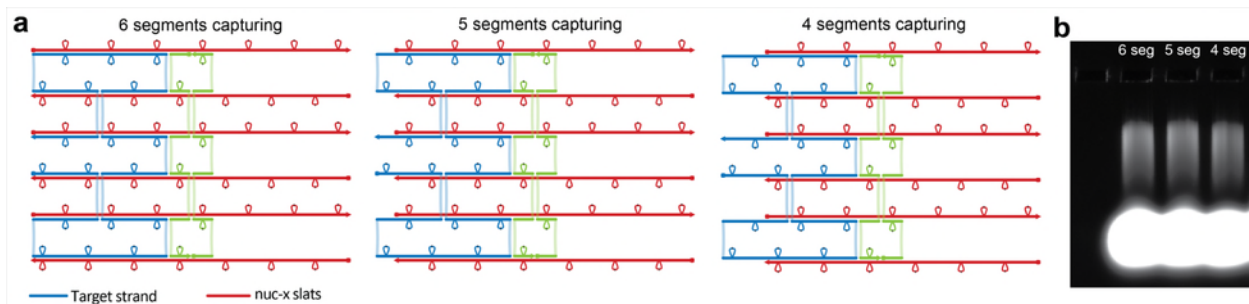


Figure S16. Nanoseed designs with varied number of segments for target capturing. a) Designed nanoseeds with 6, 5 and 4 segments for target capturing. b) AGE analyses of linear zigzag crisscross polymerization seeded by the designed nanoseeds. Conditions: 50 °C, 16 mM MgCl₂, 1 nM ultramer target, and 0.5 μM each slat, with a growth time of 2 h.

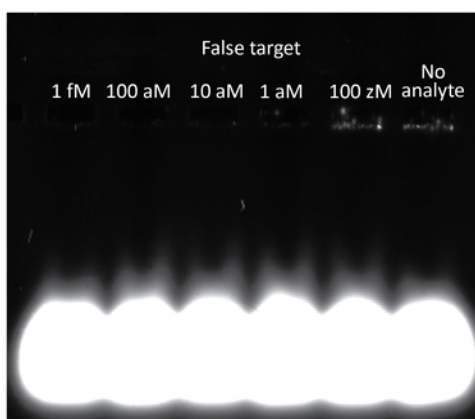


Figure S17. HypB growth using a false target strand. AGE analyses of HypB growths at varied concentrations of non-target analyte. Conditions: 50 °C, 16 mM MgCl₂, 0.1 μM each nuc-x slat, 0.125 μM each short pre-y slat, 0.25 μM each core slat, and 0.125 μM each branching nuc-y slat and adapter slat, 16 h growth time and 20 μL reaction volume. The small amount of material seen in some wells but not others is consistent with a low level of spurious nucleation on the threshold of what can be detected by gel under the stated reaction conditions.

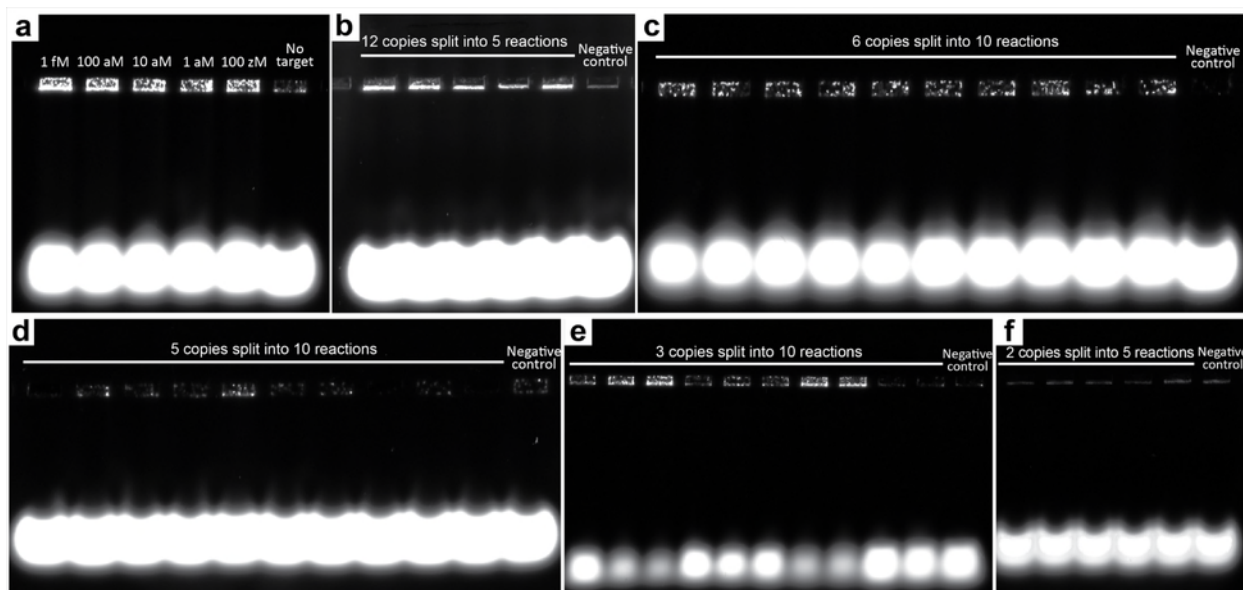


Figure S18. Amplification of targets diluted to small numbers per well. The main observation here is that when targets are diluted to below a nominal average of 1 molecule per reaction, then only some of the reaction repeats produce significant amplification, qualitatively consistent with expectations. As with Figure S17, there is a small amount of material seen in some wells but not others that we attribute to a low level of spurious nucleation on the threshold of what can be detected by gel under the stated reaction conditions. **a)** AGE analyses for the seeded HypB growths using varied target concentrations. This is a repeat of the experiment from Figure 4f, performed on a different day. We note that 100 zM in 20 μ L should correspond to an average of 1.2 copies, corresponding to a 70 % chance of being non-empty according to a Poisson distribution. Furthermore, errors in pipetting, errors due to material sticking to plastic, and errors in estimation of stock concentration can shift the actual average concentration higher or lower from the intended average concentration. **b)** AGE analyses of HypB growths with nominally 12 copies split into 5 reactions. **c)** AGE analyses of HypB growths with nominally 6 copies split into 10 reactions. **d)** AGE analyses of HypB growths with nominally 5 copies split into 10 reactions. **e)** AGE analyses of HypB growths with nominally 3 copies split into 10 reactions. **f)** AGE analyses of HypB growths with nominally 2 copies split into 5 reactions. Conditions: **a,b,f)** 50 $^{\circ}$ C, 16 mM MgCl_2 , 0.25 μ M each core slat, 0.125 μ M each branching nuc-y slat and adapter slat, and 0.1 μ M each nuc-x slat, 16 h growth time and 20 μ L reaction volume. **c-e)** 50 $^{\circ}$ C, 16 mM MgCl_2 , 0.25 μ M each core slat, 0.125 μ M each branching nuc-y slat and adapter slat, and 0.1 μ M each nuc-x slat, 16 h growth time and 10 μ L reaction volume.

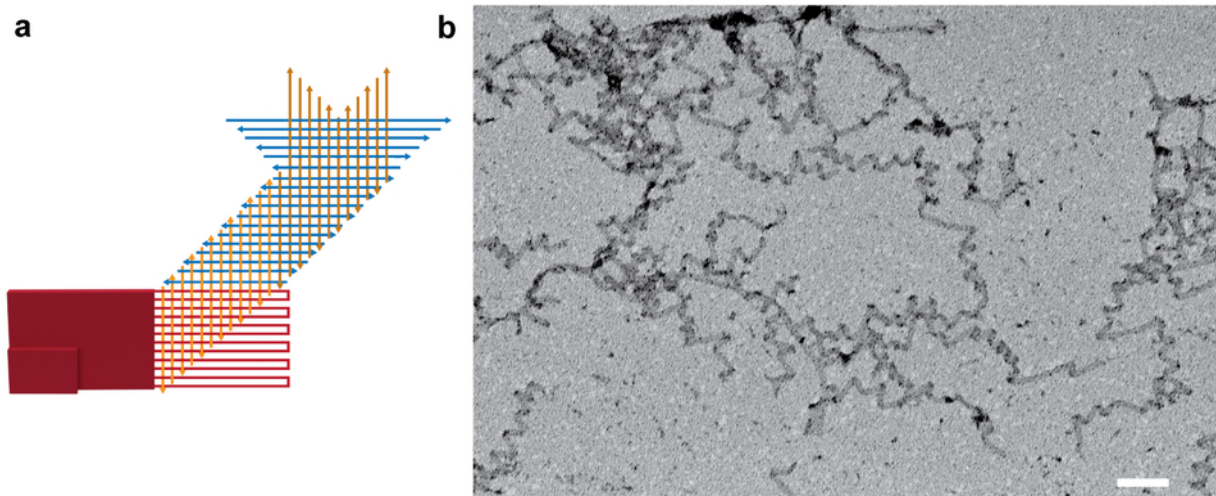


Figure S19. xy-type branching growth. **a)** Schematic illustration for xy-type branching growth. Extensions were designed on both x and y slats to allow for branching growth. **b)** TEM image of PriB growth via xy-type branching growth. Scale bar: 100 nm. Conditions: 48 °C, 14 mM MgCl_2 , 0.5 μM each slat.

Supplementary Note 1.

Our initial expectation was that HypB growth should exhibit an exponential phase during its early stage, transitioning to cubic growth as space becomes more crowded. In practice, we observed depletion of free slats that was faster than could be explained by a strictly cubic-growth model (see below). Hence, we deduce that there must be self-splitting in the HypB growth, which could lead to a sustained exponential growth phase. To support our hypothesis, we performed the following calculation.

For the HypB growth reactions conducted using 0.1 μM each nuc-x slat, 0.125 μM each short pre-y slat, 0.25 μM each core slat, 0.125 μM each branching nuc-y and adapter slat, the total slat concentration before growth is about 140 ng/ μL measured by a Nanodrop UV-Vis spectrophotometer. By utilizing an approximate average molecular weight of 307.65 g/mol for each nucleotide, the overall count of nucleotide bases in a 10 μL reaction equates to $(140 \times 10^{-9} \text{ g}/\mu\text{L}) \times (10 \mu\text{L}) / (307.65 \text{ g/mol}) \approx 4.55 \times 10^{-9} \text{ mole} = 2.74 \times 10^{15}$ nucleotides (similar to the theoretically calculated concentration). Based on the growth rate quantified in Figure 2d, the core ribbon grows ca. 250 nm per hour under the aforementioned conditions (0.25 μM each core slat). Regarding the bidirectional growth in HypB growth, following a 16 h growth period, the diameter for the particle is projected to be ca. 8 μm , resulting in an estimated volume of ca. $268.1 \mu\text{m}^3 = 2.681 \times 10^{11} \text{ nm}^3$. if each nucleotide is 1 nm^3 (i.e. 32 % weight to volume assuming 1 g/mL) as a rough first assumption, then a single particle with a diameter of 8 μm should contain 2.681×10^{11} nucleotides. Hence, the fraction of slat depletion for single molecule detection after overnight growth, without considering spurious nucleation, would be ca. $2.681 \times 10^{11} / 2.74 \times 10^{15} \approx 0.01 \%$. However, in practice, the slat-depletion fraction amounts to ca. 50 % for the detection of a single molecule following a growth period of 16 h (measured by UV-Vis absorbance of the supernatant of the reaction mixture after spinning for 10 s using a desktop minicentrifuge). We argue that such a significant depletion implies there must be self-splitting after the particle grows to a certain size, in order to produce a sustained exponential phase. Furthermore, the existence of numerous stained dots in the agarose gel pockets during the detection of 0.1–1 aM target (i.e. nominally only 1–12 copies per 20 μL volume) further supports the notion of particle self-splitting.

References

1. Minev, D.; Wintersinger, C. M.; Ershova, A.; Shih, W. M., Robust nucleation control via crisscross polymerization of highly coordinated DNA slats. *Nat. Commun.* **2021**, *12* (1), 1741.
2. Doty, D.; Lee, B. L.; Stérin, T., scadnano: a browser-based, scriptable tool for designing DNA nanostructures. *arXiv preprint arXiv:2005.11841* **2020**.
3. Zadeh, J. N.; Steenberg, C. D.; Bois, J. S.; Wolfe, B. R.; Pierce, M. B.; Khan, A. R.; Dirks, R. M.; Pierce, N. A., NUPACK: Analysis and design of nucleic acid systems. *J. Comput. Chem.* **2011**, *32* (1), 170-173.
4. Fornace, M. E.; Huang, J.; Newman, C. T.; Porubsky, N. J.; Pierce, M. B.; Pierce, N. A., NUPACK: analysis and design of nucleic acid structures, devices, and systems. **2022**.